Articles

Mycobacterium tuberculosis Mycothione Reductase: pH Dependence of the Kinetic Parameters and Kinetic Isotope Effects†

Mehul P. Patel§ and John S. Blanchard*

Department of Biochemistry, Albert Einstein College of Medicine, 1300 Morris Park Avenue, Bronx, New York 10461

Received December 22, 2000; Revised Manuscript Received February 28, 2001

ABSTRACT: The recent identification of the enzyme in *Mycobacterium tuberculosis* that catalyzes the NADPH-dependent reduction of the unique low molecular weight disulfide mycothione, mycothione reductase, has led us to examine the mechanism of catalysis in greater detail. The pH dependence of the kinetic parameters *V* and *V/K* for NADPH, NADH, and an active analogue of mycothione disulfide, des-*myo*-inositol mycothione disulfide, has been determined. An analysis of the pH profiles has allowed the tentative assignment of catalytically significant residues crucial to the mechanism of disulfide reduction, namely, the His444−Glu449 ion pair and Cys39. Solvent kinetic isotope effects were observed on *V* and V/K_{DIMSSM}, yielding values of 1.7 ± 0.2 and 1.4 ± 0.2, respectively, but not on V/K_{NADPH}. Proton inventory studies (*V* versus mole fraction of D_2O) were linear, indicative of a single proton transfer in a solvent isotopically sensitive step. Steady-state primary deuterium kinetic isotope effects on *V* have been determined using NADPH and NADH, yielding values of 1.27 ± 0.03 and 1.66 ± 0.14, respectively. The pre-steady-state primary deuterium kinetic isotope effect on enzyme reduction has values of 1.82 ± 0.04 and 1.59 ± 0.06 for NADPH and NADH, respectively. The steady-state primary deuterium kinetic isotope effect using NADH coincide with that obtained under single turnover conditions, suggesting the complete expression of the intrinsic primary kinetic isotope effect. Rapid reaction studies on the reductive half-reaction using NADPH and NADH yielded maximal rates of 129 ± 2 and 20 ± 1 s^{-1}, respectively, while similar studies of the oxidation of the two-electron reduced enzyme by mycothiol disulfide yielded a maximum rate of 190 ± 10 s^{-1}. These data suggest a unique flavoprotein disulfide mechanism in which the rate of the oxidative half-reaction is slightly faster than the rate of the reductive half-reaction.

Mycobacterium tuberculosis, and other actinomycetes, lack the ubiquitous thiol, glutathione, and its less common cyclic analogue, trypanothione, but instead produce a structurally unique thiol, mycothiol (*1*). Mycothione disulfide reductase activity has been detected in crude cell

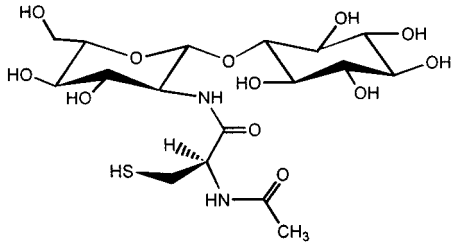

extracts of the nonpathogenic, saprophytic *Mycobacterium smegmatis*, a close phylogenetic relative of *M. tuberculosis* (*2*). The sequencing of the *M. tuberculosis* genome has aided in efforts to clone, express, and purify mycothione reductase to homogeneity, and its characterization as a member of the flavoprotein disulfide reductase family of enzymes (*3*, *4*). The enzyme catalyzes the NADPH[1]-dependent reduction of mycothione disulfide:

$$NADPH + H^+ + MSSM \rightarrow NADP^+ + 2\ MSH$$

Mycothione reductase is thought to have a similar physiological role to glutathione reductase and trypanothione reductase, namely, in the maintenance of a reducing intracellular environment and oxidative stress management. Although both glutathione and trypanothione peroxidase have been demonstrated to be dependent on the corresponding disulfide reductase to generate the respective thiol substrate (*5*, *6*), the presence of a mycothione peroxidase activity has not yet been demonstrated. The distinct structure of myco-

† This work was supported by NIH Grant GM33449 and the NIH Molecular Biophysics Training Program GM08572.

* Corresponding author: phone: (718) 430-3096; fax: (718) 430-8565. E-mail: blanchar@aecom.yu.edu.

§ Present address: SmithKline Beecham Pharmaceuticals, Inc., Dept. of Mechanistic Enzymology, King of Prussia, PA 19406.

[1] Abbreviations: MycR, mycothione reductase; DTNB, 5′,5′-dithiobis(2-nitrobenzoic acid); TEA, triethanolamine; Hepes, 4-(2-hydroxyethyl)-1-piperazineethanesulfonic acid; FAD, flavin adenine dinucleotide; FMN; flavin mononucleotide; β-NADPH, reduced β-nicotinamide adenine dinucleotide phosphate; β-NADH, reduced β-nicotinamide adenine dinucleotide; MSSM, mycothione (mycothiol disulfide); DI-MSSM, des-*myo*-inositol mycothione.

10.1021/bi0029144 CCC: $20.00
Published on Web 04/04/2001

thione and its restricted prevalence among bacteria, in particular *M. tuberculosis*, make the reductase an attractive target for the design of antitubercular drugs.

Detailed mechanistic studies of the reactions catalyzed by flavoenzymes such as glutathione and trypanothione reductase have helped further our understanding of flavoprotein chemistry (*7*−*10*). In particular, the analysis of kinetic isotope effects and the pH dependence of the kinetic parameters of several flavoproteins, including those mentioned above, have helped identify key residues that interact with the substrates and the flavin cofactor to facilitate catalysis. The determinations of the three-dimensional crystal structures of many of these enzymes have validated the mechanistic interpretations based on these kinetic experiments. The structures have driven the design of site-specific mutants that have both confirmed the chemical mechanism and in some cases allowed for a complete interchange of activities (*11*).

The initial characterization of mycothione reductase has suggested a similar mechanism to the prototypical flavoprotein disulfide reductase, glutathione reductase (*4*). The amino acid sequence of mycothione reductase is ca. 30% identical to other members of this enzyme family and possesses the catalytic redox-active cysteines and histidine−glutamate ion pair consensus regions as well as sequence motifs for NADPH and FAD binding. The reductase exhibits a Bi−Bi ping-pong kinetic mechanism where the reductive half-reaction consists of the transfer of electrons from NADPH to the active-site cysteines, via the bound FAD, to generate the anaerobically stable two-electron reduced enzyme. Subsequent transfer of the reducing equivalents from the enzymic sulfhydryls to the substrate disulfide constitutes the oxidative half-reaction (*4*).

To probe the chemistry of the reaction of mycothione reductase, we have examined the pH and isotope dependence of the kinetic parameters *V* and *V/K* for NADPH, NADH, and des-*myo*-inositol mycothione disulfide. Reduction of the enzyme under pre-steady-state conditions has allowed for the determination of the rate of enzyme reduction and the corresponding intrinsic deuterium kinetic isotope effect on hydride transfer. Rapid reaction kinetics on the oxidative half-reaction of mycothione reductase have been investigated to determine the rate of mycothione disulfide reduction by two-electron reduced enzyme.

MATERIALS AND METHODS

Materials. The procedure for the synthesis of des-*myo*-inositol mycothione disulfide has been reported (*2*). Authentic mycothione disulfide was a kind gift of Dr. Daniel J. Steenkamp, University of Cape Town Medical School, South Africa. d-[1-^{2}H]Glucose (97 atom % ^{2}H), oxidized pyridine nucleotides, *Leuconostoc mesenteriodes* (type XXIV) glucose-6-phosphate dehydrogenase, yeast hexokinase, ATP, and all buffers were purchased from Sigma. Deuterated water (D_2O) was purchased from Cambridge Isotope Laboratories.

Cloning and Purification of Hexahistidyl-Tagged Mycothione Reductase. The expression vector for mycothione reductase in *M. smegmatis* mc^{2}155 was modified by engineering a hexahistidyl tag at the carboxyl terminus of the *mtr* gene open reading frame by PCR methods. This was performed to completely, and rapidly, separate the recombinant *M. tuberculosis* enzyme from the extant *M. smegmatis* reductase. The His_6-tag was placed immediately preceding the termination codon, by use of the reverse oligonucleotide 5′-GCG-GAT-CCG-TCA-ATG-ATG-ATG-ATG-ATG-ATG-ACG-CAG-GCC-AAG-CAG-CGC-3′. The PCR and expression conditions of the His_6-tagged mycothione reductase were as described previously (*4*). The soluble extract of *M. smegmatis* mc^{2}155 harboring the gene (pMV261-MycRHis_6) encoding for a carboxy-terminal hexahistidyl-tagged mycothione reductase was prepared as described (*4*). The cell-free extract was loaded onto a 20 mL Ni^{2+}-chelate (Pharmacia) column equilibrated with buffer A (20 mM TEA-HCl, pH 7.6) at 4 °C. The column was washed with 50 mL of buffer A followed by 50 mL of buffer A containing 25 mM imidazole. This was followed by a 100 mL, 25−250 mM linear imidazole gradient which eluted the homogeneous protein at ca. 125 mM imidazole. The purified His_6-tagged mycothione reductase was immediately dialyzed overnight against 20 mM TEA-HCl, pH 7.6, at 4 °C.

Preparation of Isotopically Labeled Pyridine Nucleotides. Pyridine nucleotides stereospecifically deuterated at the C4S position were prepared enzymatically as previously described (*12*). The reduced, deuterated nucleotides were purified using a MonoQ (Pharmacia) anion exchange column as previously described (*12*). An A_{260}/A_{340} absorbance ratio of ≤ 2.3 was used to assess the purity of the reduced nucleotides. The concentration of the purified, reduced nucleotides was determined by enzymatic end-point assays using yeast glutathione reductase.

Steady-State Primary Deuterium Kinetic Isotope Effects. Initial rates of the des-*myo*-inositol mycothione-dependent reduction by pyridine nucleotides were measured in 50 mM HEPES, pH 7.6, at 25 °C using 0.5 mM disulfide and varying concentrations of the [4*S*-4-^{2}H]-reduced pyridine nucleotides. Pyridine nucleotide oxidation was monitored at 340 nm using an extinction coefficient of 6220 M^{-1} cm^{-1}.

Rapid Reaction Kinetics. Enzyme reduction and oxidation were monitored using an Applied Photophysics SX.17MV stopped-flow spectrophotometer (mixing dead time = 1.5 ms) at 25 °C. Mycothione reductase (30 μM) in 20 mM TEA-HCl, pH 7.8, was made anaerobic by purging the solution with nitrogen for 45 min. NADPH(D) and NADH(D) samples were made anaerobic by bubbling the solutions with nitrogen for 15 min. The solutions were transferred into the drive syringes with Hamilton gastight syringes. The procedure for generating an anaerobic solution of two-electron reduced enzyme was similar to that reported for glutathione reductase (*13*). Enzyme reduction and oxidation was monitored at 530 nm for 10 s on a log time scale.

Solvent Kinetic Isotope Effects and Proton Inventory. Solvent kinetic isotope effects on *V* and *V/K* for des-*myo*-inositol mycothione disulfide were determined by measurement of the initial rates of reduction at 340 nm using variable disulfide substrate concentrations at a saturating concentration of NADPH (0.1 mM) at 25 °C. The buffers were composed of 50 mM HEPES, pH(D) 7.6 [where $pD = pH_{measured} + 0.4$ (*14*)] prepared in H_2O and 99.8% D_2O by titrating with KOH dissolved in H_2O or D_2O. The proton inventory for the mycothione reductase reaction was determined at pH(D) 7.6 by measuring the initial velocities in triplicate at various mole fractions of D_2O using a saturating concentration of NADPH and 0.8 mM DIMSSM ($2\times K_{DIMSSM}$). Values of *V* and *V/K*

at 0 and 98.6% D_2O were obtained by fitting the initial velocity data at variable disulfide substrate concentration to eq 1.

pH Profiles. The buffers used for the pH studies were dissolved in Millipore filtered water and adjusted to the desired pH by titrating their acid forms with KOH at a final stock concentration of 500 mM. The reactions were performed in the following buffers (100 mM buffer) and pH values: MES (5.5−6.3), PIPES (6.1−7.0), HEPES (7.0−8.0), TAPS (7.8−8.9), and CHES (9.0−10.0). Initial velocities of the reaction catalyzed by mycothione reductase at the stated pH values were measured by varying the concentration of one of the substrates while maintaining the other at a fixed saturating level. The kinetic parameters *V* and *V/K* for des-*myo*-inositol mycothione disulfide were determined by varying the concentration of the disulfide between 0.1 and 1 mM at a saturating concentration of NADPH (100 μM). The kinetic parameters *V*, V/K_{NADPH}, and V/K_{NADH} were determined by varying the concentration of NADPH between 5 and 50 μM, and NADH between 50 and 200 μM, at a subsaturating concentration of des-*myo*-inositol mycothione disulfide ($2\times K_M$).

Data Analysis. Kinetic data were fitted to the appropriate rate equations by using the nonlinear regression function of SigmaPlot (Jandel Scientific). Individual saturation curves were fitted to eq 1 to determine the kinetic parameters (*V* and *V/K*) for the substrates.

$$v = VA/(K + A) \quad (1)$$

The steady-state primary kinetic isotope effects on hydride transfer were determined by fitting the experimental initial velocity values to eqs 2−4.

$$v = VA/[K + A(1.0 + F_iE_V)] \quad (2)$$

$$V = VA/[K(1.0 + F_iE_{V/K}) + A] \quad (3)$$

$$v = VA/[K(1.0 + F_iE_{V/K}) + A(1.0 + F_iE_V)] \quad (4)$$

where isotope effects are exhibited on *V* only, on *V/K* only, or on both *V* and *V/K*, respectively. In eqs 1−4, *A* is the variable substrate concentration, F_i is the fraction of deuterium label in the reduced pyridine nucleotide substrate ($F_i = 0$ and 1 for hydrogen- and deuterium-containing substrates, respectively), $E_V = {}^DV - 1$. and $E_{V/K} = {}^DV/K - 1$. For each case, the most appropriate fit was chosen according to the lowest standard errors of the fitted parameters.

To construct the pH profiles, the kinetic parameters *V* and *V/K* for the substrates were determined between pH 5.5 and pH 10.3, and the p*K* values were determined by fitting the values of the kinetic parameters at each pH value to eqs 5−7. Plots in which the log of the parameter decreased at acidic and basic pH with slopes of 1 and −1, were fitted to eq 5. pH profiles in which the log of the plotted parameter decreased at acidic pH with a slope of 1 were fitted to eq 6. pH profiles that showed a decrease in log *V* or *V/K* at basic pH with a slope of −1 were fitted to eq 7. In eq 5−7, *y* is the parameter to be fitted and *C* is the pH-independent plateau value.

$$\log y = \log [C/(1.0 + [H^+]/K_a + K_b/[H^+])] \quad (5)$$

$$\log y = \log [C/(1.0 + [H^+]/K_a)] \quad (6)$$

$$\log y = \log [C/(1.0 + K_b/[H^+])] \quad (7)$$

Data from the stopped-flow experiments were best fitted to a single exponential using the Applied Photophysics software. The fitted rate constants (k_{obs}) for enzyme reduction were plotted versus pyridine nucleotide concentration, and the fitted rate constants for two-electron reduced enzyme oxidation by disulfide were plotted versus mycothione concentration. All observed rate constants increase hyperbolically with increasing substrate concentration and were fitted to eq 8. The pre-steady-state kinetic isotope effects on

$$k_{obs} = k[S]/(K_d + [S]) \quad (8)$$

enzyme reduction were obtained by fitting the observed rate constants to eq 9:

$$k_{obs} = kS/([K_d + S][1.0 + F_i({}^Dk - 1)]) \quad (9)$$

where *S* is the variable substrate concentration, F_i is the fraction of deuterium label in the reduced pyridine nucleotide substrate ($F_i = 0$ or 1), and ${}^Dk$ is the kinetic isotope effect on the rate constant *k*.

RESULTS

pH Profiles of the Kinetic Parameters. The pH profiles of the kinetic parameters using NADPH, NADH, and des-*myo*-inositol mycothione disulfide are shown in Figure 1. The pH profile of log *V* (Figure 1, panel a) for mycothione reduction is dependent on two ionizing groups exhibiting p*K* values of 6.8 ± 0.2 and 9.1 ± 0.2 whose protonation and deprotonation, respectively, diminish activity. Figure 1, panel b, shows the pH dependence of V/K_{DIMSSM}, with V/K_{DIMSSM} decreasing at low pH values as a single group exhibiting a p*K* value of 6.5 ± 0.2 is protonated. The pH dependence of *V/K* for NADPH is shown in Figure 1, panel c. V/K_{NADPH} decreased at low and high pH as two ionizing groups exhibiting p*K* values of 7.0 ± 0.2 and 9.2 ± 0.2 are protonated and deprotonated, respectively. The pH dependence of V/K_{NADH} was determined (Figure 1, panel d) and decreases as a single group exhibiting a p*K* value of 9.4 ± 0.2 is deprotonated.

Steady-State Primary Deuterium Kinetic Isotope Effects. Primary deuterium kinetic isotope effects were determined using varying concentrations of NADPH and NADH at a fixed concentration of mycothione at pH 7.6. The kinetic parameters determined for the nucleotide substrates, and the corresponding isotope effects are presented in Table 1. A small primary deuterium kinetic isotope effect was observed on *V* (1.27 ± 0.03) using [4S-4-^{2}H]NADPH as the reductant, with no effect on *V/K*. Larger and statistically equivalent values of ${}^DV$ (1.7 ± 0.1) and ${}^DV/K$ (1.6 ± 0.3) were observed using NADH.

Solvent Kinetic Isotope Effects and Proton Inventory. Solvent kinetic isotope effects and the proton inventory on mycothione reduction were determined at pH(D) 7.6. The values of ${}^{D_2O}V$ and ${}^{D_2O}V/K$ determined using variable concentrations of NADPH were 1.6 ± 0.1 and 1.2 ± 0.2, respectively (data not shown). Solvent kinetic isotope effects on *V* and V/K_{DIMSSM} were observed with values of 1.7 ± 0.2

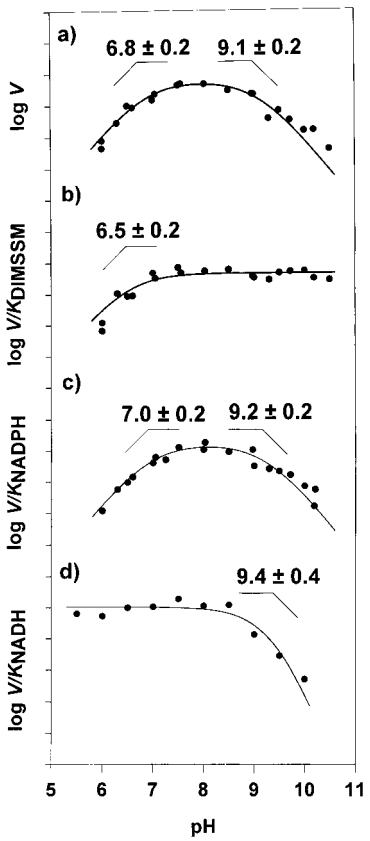

FIGURE 1: The pH dependence of the kinetic parameters *V* and *V/K* for des-*myo*-inositol mycothione disulfide, NADPH, and NADH. (a) The *V* pH profile shows two enzymatic groups with p*K*'s of 6.8 ± 0.2 and 9.1 ± 0.2 whose protonation and deprotonation, respectively, diminish activity. (b) The V/K_{DIMSSM} profile shows a single group with a p*K* of 6.5 ± 0.2 whose protonation abolishes activity. (c) The V/K_{NADPH} profile indicates two groups with p*K*'s of 7.0 ± 0.2 and 9.2 ± 0.2 whose protonation and deprotonation, respectively, reduces binding. (d) The V/K_{NADH} profile reveals a single group with a p*K* of 9.4 ± 0.4 that decreases binding. The experimental points are shown and the solid lines represent the fit of the data to eq 5−7 according to the type of pH-dependent behavior.

and 1.4 ± 0.2, respectively (Figure 2). The disulfide substrate DTNB does not exhibit a solvent kinetic isotope effect (data not shown). To assess the number of protons involved in the solvent isotopically sensitive step, a proton inventory analysis was conducted. A linear relationship between *V* and the mole fraction of D_2O was observed (Figure 2, insert).

Rapid Reaction Kinetics on the Reductive and Oxidative Half-Reaction. The absorbance traces for the reduction of mycothione reductase by 0.5 mM NADPH or [4*S*-4-^{2}H]-NADPH are shown in Figure 3. A single-exponential phase was observed at 530 nm corresponding to the formation of the stable, two-electron reduced enzyme using either NADPH or NADH and the plots of k_{obs} versus [NADPH] indicated saturation behavior. The plots of reciprocal rate constants versus the reciprocal of the NADPH and NADH concentrations are shown in Figure 4. Maximum rates of 129 ± 2 and 20 ± 1 s^{-1} were determined for NADPH and NADH, respectively. The deuterium kinetic isotope effects under pre-steady-state conditions were calculated using eq 9, and values of 1.82 ± 0.04 and 1.59 ± 0.06 were obtained[2] for NADPH and NADH, respectively.

The oxidation of two-electron reduced mycothione reductase by mycothione disulfide at 25 °C is monophasic (Figure 5, panel A). The oxidative half-reaction of mycothione reductase has a maximum rate of 190 ± 10 s^{-1} extrapolated to saturating disulfide substrate concentration (Figure 5, panel B).

DISCUSSION

The isotopic analyses of flavoprotein disulfide reductases have allowed for a detailed characterization of the rate-limiting nature of chemical steps in these enzymatic reactions. The archetypal disulfide reductase, glutathione reductase, has been physically, kinetically, and structurally analyzed in detail and serves as a useful model for mycothione reductase (*9*, *10*, *15*−*17*). From considerations of primary sequence homology and initial kinetic studies (*4*), mycothione reductase has many of the characteristics associated with flavoprotein disulfide reductases.

pH Studies. The ionization behavior of enzyme groups on mycothione reductase and those on the substrates, NADPH and des-*myo*-inositol mycothione, reflects critical functionalities that are important for both binding and catalysis. The "bell-shaped" pH profile for *V* differs from that observed for glutathione or trypanothione reductase in that the protonation of an enzyme group (p*K* value of 6.8) does not affect the maximal velocity of these homologous enzymes (*8*, *17*). In the case of both glutathione and trypanothione reductase, a wealth of evidence supports the reoxidation of the two-electron-reduced enzyme as the rate-limiting half-reaction, while for mycothione reductase, we have evidence that the two half-reactions occur with very similar rates (see below). This suggests that the ionization behavior of groups in both half-reactions must be considered. The log *V* pH profiles of both human erythrocyte glutathione reductase and *Trypanosoma congolense* trypanothione reductase decrease as groups exhibiting p*K* values of 9.0 and 9.5, respectively, are deprotonated (*8*, *17*). In both cases, this group has been assigned to the histidine−glutamate ion pair from the neighboring monomer, which donates a proton to the first product thiolate anion accompanying the disulfide interchange reaction (*19*, *20*). Evidence supporting this assignment also comes from site-specific mutants of *Escherichia coli* glutathione reductase where the histidine was replaced with an alanine, resulting in a shift in the p*K* from ca. 9.2 for the wild-type enzyme to 7.6 for the mutant (*13*). We do not observe this group in the V/K_{DIMSSM} profile (see below), suggesting that in this case, the protonation of the His444−Glu449 ion-pair is required during enzyme reduction, presumably to stabilize the thiolate anions formed in the reductive half-reaction. The group exhibiting the p*K* value of 6.8 may be that of Cys39. During enzyme reduction, the Cys39−Cys44 disulfide is cleaved to generate the dithiol(ate), and Cys44 remains ionized as evidenced by its strong charge transfer interaction with FAD. Protonation of Cys39 might slow the rate of enzyme reduction and would similarly be expected to significantly reduce the rate of the oxidative

[2] The data in Figure 4 were fitted to an equation that assumes equivalent isotope effects on the slope and intercept (i.e., no isotope effect on K_d). Fitting the data to an equation that allows for different isotope effects on k_{red} and k_{red}/K_d yields values of k_{red} for NADPH and NADH of 1.70 ± 0.05 and 2.06 ± 0.07 as compared to 1.82 ± 0.04 and 1.59 ± 0.06 reported in the text from the lines shown fitted to eq 9. These small differences do not change our mechanistic interpretations.

Table 1: Steady-State Primary Deuterium and Solvent Kinetic Isotope Effects

nucleotide substrate	k_{cat} (s^{-1})[a]	K_M (μM)	^{D}V[a]	$^{D}(V/K)$[a]	^{D_2O}V[b]	$^{D_2O}(V/K_{DIMSSM})$[b,c]
β-NADPH	64 ± 2	7 ± 1	1.27 ± 0.03	1.0	1.7 ± 0.2	1.4 ± 0.2
β-NADH	23 ± 1	48 ± 7	1.7 ± 0.1	1.6 ± 0.3	nd[d]	nd[d]

[a] Determined using 500 μM MSSM and a variable pyridine nucleotide concentration. [b] Determined using 100 μM β-NADPH and a variable DI-MSSM concentration. [c] A solvent kinetic isotope effect on V/K_{NADPH} (1.2 ± 0.2) was observed. [d] Not determined.

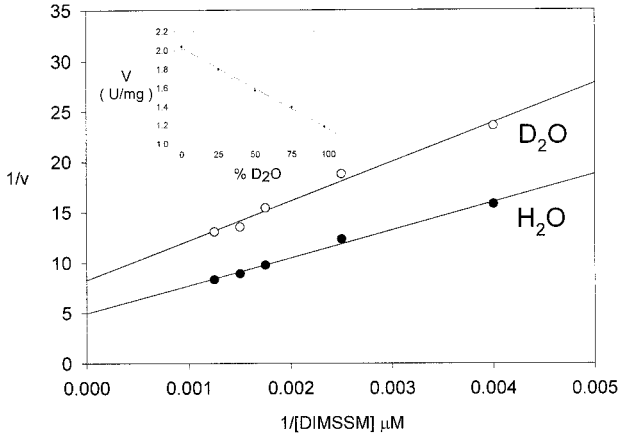

FIGURE 2: Solvent kinetic isotope effect and proton inventory of the reaction catalyzed by mycothione reductase. The reciprocal plot of the steady-state initial velocity data using H_2O (●) and D_2O (○). The data were fit to eq 4 yielding solvent kinetic isotope effects on V and V/K_{DIMSSM} of 1.7 ± 0.2 and 1.4 ± 0.2, respectively. A solvent kinetic isotope effect was not observe for V/K_{NADPH}. Inset: a linear fit to the data of V versus mole fraction D_2O was obtained.

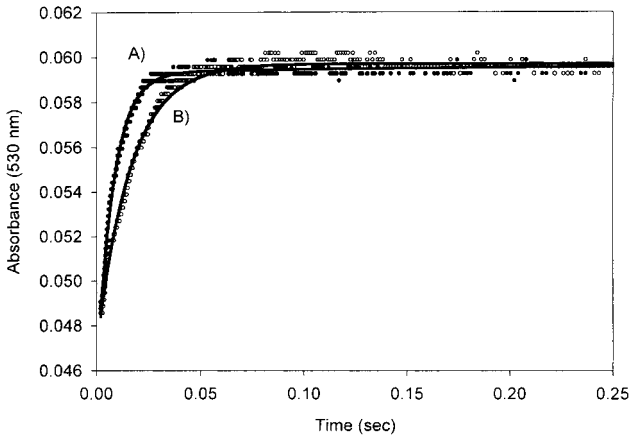

FIGURE 3: Representative stopped-flow traces monitoring the reduction of mycothione reductase at 530 nm using 0.50 mM NADPH (A) and [4S-4-^{2}H] NADPH (B). The smooth curves represent single-exponential fits of the experimental traces with a rate of 126 ± 1 and 62 ± 1 s^{-1} for the protiated and deuterated substrate, respectively.

half-reaction, since in this half-reaction, Cys39 functions as a nucleophile in disulfide substrate reduction.

The pH profile for *V/K* for the disulfide substrate, des-*myo*-inositol mycothione, decreases as a single group with a p*K* value of 6.5 is protonated and is pH-independent in the basic region (Figure 1, panel b). As there are no ionizable groups on the disulfide substrate, we suggest that the ionized, thiolate form of Cys39, which initiates substrate disulfide cleavage is this group. It is likely that this cysteine is the residue modified by cysteine alkylating agents, resulting in the specific inhibition of disulfide reductase activity (*4*).

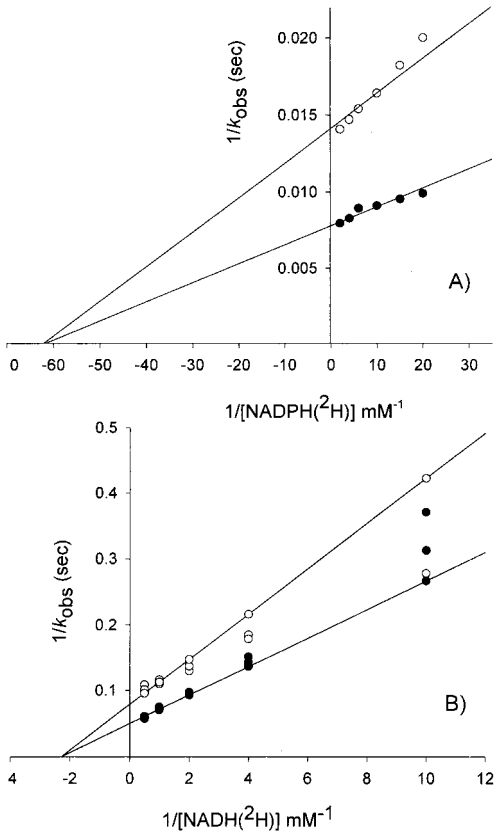

FIGURE 4: Pre-steady-state kinetic isotope effects of the reductive half-reaction of mycothione reductase. Reciprocal plot of k_{obs} versus (A) NADPH (●) and [4S-4-^{2}H]NADPH (○) and (B) NADH (●) and [4S-4-^{2}H]NADH (○). A value of 1.82 ± 0.04 and 1.59 ± 0.06 for ^{D}k was calculated for NADPH and NADH, respectively. The maximum rate of reduction (k_{red}) for NADPH and NADH is 128 ± 2 and 20 ± 1 s^{-1}, respectively.

The *V/K* pH profile for NADPH decreases at both high and low pH values, as a result of the ionization of groups exhibiting p*K* values of 7.0 and 9.2 (Figure 1, panel c). In contrast, the pH profile for V/K_{NADH} reveals pH-independent behavior at low pH but decreases in the basic region as a single group exhibiting a p*K* value of 9.4 is deprotonated (Figure 1, panel d). This difference suggests that the 2′-phosphate moiety of NADPH is the ionizing group observed at low pH values in the V/K_{NADPH} profile. The solution p*K* of the 2′-phosphate moiety of NADPH has been reported as 6.5 (*22*). The group whose deprotonation at high pH values affects the *V/K* value of both NADPH and NADH is unlikely to be either Arg 203 or Arg 209, homologous residues in mycothione reductase to those in glutathione reductase that make contacts with the 2′-phosphate moiety of NADPH (*21*). An arginine residue (Arg291) has been observed in human glutathione reductase interacting with the pyrophosphate group present in both NADPH and NADH (*21*). The homologous Arg256 in mycothione reductase may

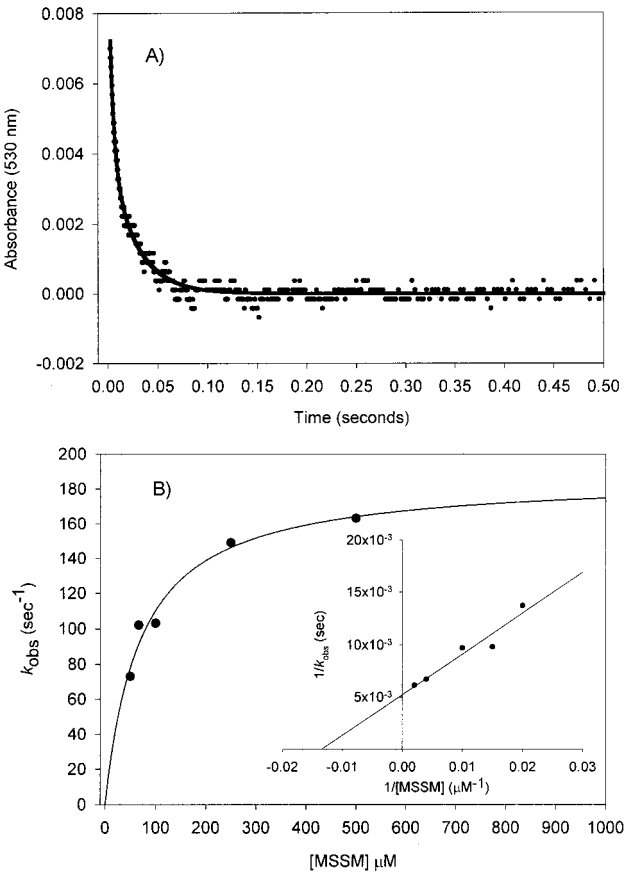

FIGURE 5: Pre-steady-state kinetics on the oxidative half-reaction of mycothione reductase. (A) Oxidation of 25 μM two-electron reduced mycothione reductase with 50 μM mycothione disulfide in 20 mM TEA-HCl, pH 7.6, 25 °C measured at 530 nm. The experimental traces were fitted to to a single exponential (solid curve) with a rate of 73 ± 1 s^{-1}. (B) The maximum rate of two-electron reduced enzyme oxidation is 190 ± 11 s^{-1}. Inset: reciprocal plot of k_{obs} versus mycothione disulfide concentration.

represent the group observed at high pH values in these two pH profiles.

Steady-State Kinetic Isotope Effects. Small steady-state primary deuterium kinetic isotope effects are observed on *V* using NADPH as the variable substrate. The lack of a primary deuterium kinetic isotope effect on V/K_{NADPH} suggests that NADPH is sticky. The larger, and equivalent, primary deuterium kinetic isotope effects on *V* and *V/K* observed with NADH indicates that this substrate is not kinetically sticky, and the isotope-sensitive hydride transfer step has become more rate-limiting. These steady-state results are quantitatively supported by the pre-steady-state results discussed below.

Modest solvent kinetic isotope effects of 1.7 and 1.4 on ^{D_2O}V and $^{D_2O}V/K_{DIMSSM}$, respectively, were observed. The observation that $^{D_2O}V/K_{NADPH}$ is 1.2 ± 0.2 suggests that the protonation of His444 does not occur in a kinetically significant step in the reductive half-reaction. The plot of *V* as a function of mole fraction of D_2O yields a linear relationship indicating that a single proton is involved in the isotope-sensitive step. The solvent isotopically sensitive proton transfer must occur in the oxidative half-reaction, presumably during protonation of the product thiolate by the active site acid, His444. Similar solvent kinetic isotope effects have been reported for other flavoprotein disulfide reductases (*8*, *17*).

Pre-Steady-State Kinetic Analysis. Three distinct chemical intermediates have been proposed to occur in the reductive half-reaction of flavoprotein disulfide reductases (*13*). The first of these is a rapidly formed E_{ox}-FAD-NADPH charge-transfer complex, the second is a transient E_{ox}-FADH$^-$-NADP$^+$ species, and the third is the thiol-flavin charge-transfer complex with the characteristic absorbance at ca. 530 nm formed by electron transfer from FADH$^-$ to the disulfide. The pre-steady-state kinetic analysis of the reductive half-reaction was performed using both NADPH and NADH. Reduction of the enzyme with NADPH under single turnover conditions occurs via single-exponential kinetics with a rapid increase in absorbance at 530 nm ($k_{red,max}$ = 129 ± 2 s^{-1}), representing the formation of the stable, two-electron reduced form of the enzyme. Under similar experimental conditions, enzyme reduction by NADH occurs with a maximum extrapolated rate of 20 ± 1 s^{-1}. An extrapolated maximal value of 190 ± 10 s^{-1} for the oxidation of the two-electron reduced enzyme by mycothione is consistent with both the overall steady-state k_{cat} and other criteria (discussed below).

The primary deuterium kinetic isotope effect under pre-steady-state conditions using either NADPH or NADH are similar (1.8 and 1.6, respectively). The similarity of these values to those determined for the steady-state primary deuterium kinetic isotope effect on both *V* and *V/K* using NADH suggests an intrinsic primary deuterium kinetic isotope effect on hydride transfer from reduced pyridine nucleotides to flavin of ca. 1.7. This value can be compared to the intrinsic kinetic isotope effect of 1.7 reported for human erythrocyte glutathione reductase and 2.7 for yeast glutathione reductase and trypanothione reductase (*7*, *8*, *16*).

Proposed Kinetic Model and Chemical Mechanism. A minimal kinetic model for the analysis of the kinetic isotope effects is shown below:

$$E_{ox} + \text{NAD(P)H} \underset{k_2}{\overset{k_1}{\rightleftharpoons}} E_{ox}\text{-NAD(P)H} \underset{k_4^*}{\overset{k_3^*}{\rightleftharpoons}} E_{red}\text{-NAD(P)}^+ \underset{k_6}{\overset{k_5}{\rightleftharpoons}} E_{red} + \text{NAD(P)}^+$$

$$E_{red} + \text{MSSM} \underset{k_8}{\overset{k_7}{\rightleftharpoons}} E_{red}\text{-MSSM} \underset{k_{10}}{\overset{k_9}{\rightleftharpoons}} E_{ox}\text{-2 MSH} \xrightarrow{k_{11}} E_{ox} + \text{2 MSH}$$

A value of 7 s^{-1} was previously reported (*4*) for k_{cat} using NADPH and MSSM. Using the more rapid affinity purification method developed for these studies, steady-state k_{cat} values of 64 ± 2 and 23 ± 1 s^{-1} have been determined using NADPH and NADH, respectively. For a ping-pong mechanism, the relationship between the rate of the overall reaction and two-half reactions is

$$1/k_{cat} = 1/k_{red} + 1/k_{ox}$$

For NADPH, the determined values of k_{cat} (64 s^{-1}) and k_{red} (129 s^{-1}) allow us to calculate a value of 127 s^{-1} for k_{ox}, a value consistent with the measured value of 190 ± 10 s^{-1}. For NADH, the statistically equivalent values of k_{cat} (23 s^{-1}) and k_{red} (20 s^{-1}) suggest that the reductive half-reaction is completely rate-limiting, in support of the equivalence of ^DV, $^DV/K_{NADH}$, and $^Dk_{red}$ determined using NADH.

Scheme 1: Proposed Chemical Mechanism for *M. Tuberculosis* Mycothione Reductase

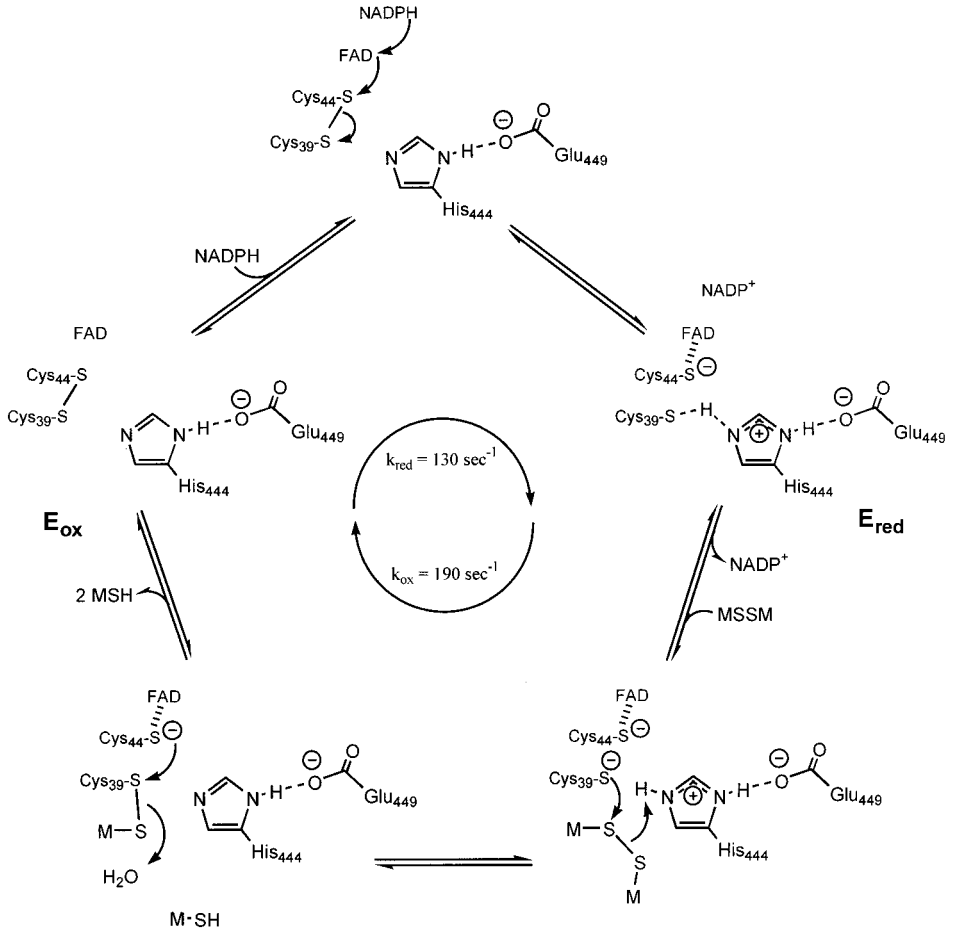

The equations for the expression of the primary deuterium kinetic isotope effect on *V* and *V/K* were derived using the net rate constants method (*24*) and are

$$^{D}(V/K)_{NAD(P)H} = (^{D}k_3 + c_f + c_r{}^{D}K_{eq})/(1 + c_f + c_r)$$

$$^{D}V = (^{D}k_3 + c_{Vf} + c_r{}^{D}K_{eq})/(1 + c_{Vf} + c_r)$$

where $^{D}k_3$ is the intrinsic primary deuterium kinetic isotope effect on the isotope-sensitive hydride transfer step, $c_f = k_3/k_2$, $c_r = k_4/k_5$, $c_{Vf} = k_3/k_5 + k_3/k_{11} + k_3/k_9(1.0 + k_{10}/k_{11})$, and $^{D}K_{eq} = k_{3H}k_{4D}/k_{3D}k_{4H} = 0.98$ (*25*). The values of the commitment factors, c_f (forward for *V/K*), c_r (reverse for *V* and *V/K*), and c_{Vf} (forward for *V*) affect the magnitude of the observed primary kinetic isotope effect on *V* and *V/K*. The presence of a primary deuterium kinetic isotope effect on *V* and a lack of an effect on *V/K* using NADPH as reductant indicate significant forward and/or reverse commitment factors for this substrate. The observed values of 1.0 for $^{D}V/K_{NADPH}$, and 1.6 for $^{D}V/K_{NADH}$, suggest that the c_f for NADPH is higher than NADH, reflecting both higher steady-state affinity (cf. K_m values, Table 7) and the higher maximal velocity of NADPH. Exactly this type of isotopic behavior has been observed with the related glutathione reductase (*9*). The steady-state value of 1.3 for $^{D}V_{NADPH}$, and the value of the pre-steady-state kinetic isotope effect on the reductive half-reaction of 1.6−1.8, can be used with eq 11 to calculate a $c_{Vf} + c_r$ range of 1.0−1.7. The experimentally determined values for k_{red} (129 s^{-1}) and k_{ox} (190 s^{-1}) which approximate k_3 and k_9, respectively, predict a c_{Vf} value of 0.7 if only the ratios of these rate constants (k_3/k_9) contributed to lowering the observed isotope effect from the intrinsic effect. This indicates that terms other than k_3/k_9 are contributing to the magnitude of c_{Vf} or that c_r may not have a unit value due to slow release of $NADP^+$ (*26*).

The studies reported here allow us to present a more detailed mechanism for mycothione reductase (Scheme 1). The strong primary sequence, tertiary structural, and functional homology observed between flavoprotein disulfide reductases strengthen the interpretation of the results of the studies on mycothione reductase presented here. The binding of NAD(P)H is likely to be very fast, while hydride transfer from NAD(P)H to the tightly bound FAD and subsequent electron transfer to the active site occurs at a rate of 129 s^{-1}. This rate constant can be compared with 110 s^{-1} for the reduction of *E. coli* glutathione reductase (*13*). The two-electron reduced enzyme is thought to be stabilized by the protonated His444, which shares a proton with the distal cysteine, Cys39.

The oxidative half-reaction involves binding of mycothione disulfide to the two-electron reduced enzyme. The Cys39 thiolate is shown attacking the substrate disulfide to form a mixed enzyme−substrate disulfide with release of the first thiol product MSH. The participation of the ionized form of Cys39 in this step is supported by the pH dependence of *V* and V/K_{DIMSSM}. The solvent kinetic isotope effects on *V* and V/K_{DIMSSM} suggest that a solvent-derived proton is transferred during disulfide substrate cleavage, and we show His444,

functioning as the general acid in this step, as proposed for glutathione reductase previously (*17*). The final step involves reformation of the enzymic disulfide and release of the second molecule of product thiolate.

The chemical mechanism of mycothione reductase presented here bears obvious similarity to those proposed for related flavoprotein disulfide reductases (*27*). The major difference observed is the similarity in the rates of the reductive and oxidative half-reaction for mycothione reductase. In other disulfide reductases, the reductive half-reaction is invariably faster than the oxidative half-reaction. Whether this kinetic difference provides a physiological advantage to this intracellular pathogen is unknown at this time.

ACKNOWLEDGMENT

The authors thank Dr. Daniel J. Steenkamp for the generous gift of mycothione disulfide and Drs. Carolyn Koo and Xianzhi Zhou for technical assistance.

REFERENCES

1. Sakuda, S., Zhou, Z.-Y., and Amada, Y. (1994) *Biosci. Biotechnol. Biochem. 268*, 255−263.
2. Patel, M. P., and Blanchard, J. S. (1998) *J. Am. Chem. Soc. 124*, 11538−11539.
3. Cole, S. T., Brosch, R., Parkhill, J., Garnier, T., Churcher, C., Harris, D., Gordon, S. V., Eiglmeier, K., Gas, S., Barry, C. E. 3., Tekaia, F., Badcock, K., Basham, D., Brown, D., Chillingworth, T., Connor, R., Davies, R., Devlin, K., Feltwell, T., Gentles, S., Hamlin, N., Holroyd, S., Hornsby, T., Jagels, K., Barrell, B. G., et al. (1998) *Nature 393*, 537−44.
4. Patel, M. P., and Blanchard, J. S. (1999) *Biochemistry 38*, 11827−33.
5. Tetaud, E., and Fairlamb, A. H. (1998) *Mol. Biochem. Parasitol. 96*, 111−23.
6. Yoshimura, S., Onozawa, T., Mizoguchi, J., Suemizu, H., Moriuchi, T., and Watanabe, K. (1990) *Nucleic Acids Symp. Ser. 22*, 71−2.
7. Huber, P. W., and Brandt, K. G. (1980) *Biochemistry 19*, 4569−75.
8. Leichus, B. N., Bradley, M., Nadeau, K., Walsh, C. T., and Blanchard, J. S. (1992) *Biochemistry 31*, 6414−20.
9. Vanoni, M. A., Wong, K. K., Ballou, D. P., and Blanchard, J. S. (1990) *Biochemistry 29*, 5790−6.
10. Wong, K. K., Vanoni, M. A., and Blanchard, J. S. (1988) *Biochemistry 27*, 7091−6.
11. Bradley, M., Bucheler, U. S., and Walsh, C. T. (1991) *Biochemistry 30*, 6124−7.
12. Orr, G. A., and Blanchard, J. S. (1984) *Anal. Biochem. 142*, 232−234.
13. Rietveld, P., Arscott, L. D., Berry, A., Scrutton, N. S., Deonarain, M. P., Perham, R. N., and Williams, C. H., Jr. (1994) *Biochemistry 33*, 13888−95.
14. Schowen, R. L. (1977) in *Isotope Effects in Enzyme Catalyzed Reactions* (Cleland, W. W., O'Leary, M. H., and Northrop, D. B., Ed.) pp 64−99, University Park Press, Baltimore, MD.
15. Pai, E. F., and Schulz, G. E. (1983) *J. Biol. Chem. 258*, 1752−7.
16. Sweet, W. L., and Blanchard, J. S. (1991) *Biochemistry 30*, 8702−9.
17. Wong, K. K., and Blanchard, J. S. (1989) *Biochemistry 28*, 3586−90.
18. Karplus, P. A., and Schulz, G. E. (1989) *J. Mol. Biol. 210*, 163−80.
19. Janes, W., and Schulz, G. E. (1990) *Biochemistry 29*, 4022−30.
20. Kuriyan, J., Krishna, T. S., Wong, L., Guenther, B., Pahler, A., Williams, C. H., Jr., and Model, P. (1991) *Nature 352*, 172−4.
21. Pai, E. F., Karplus, P. A., and Schulz, G. E. (1988) *Biochemistry 27*, 4465−74.
22. Mas, M. T., and Colman, R. F. (1984) *Biochemistry 23*, 1675−83.
23. Sullivan, F. X., Shames, S. L., and Walsh, C. T. (1989) *Biochemistry 28*, 4986−92.
24. Cleland, W. W. (1979) *Methods Enzymol. 63*, 103−38.
25. Cleland, W. W. (1980) *Methods Enzymol. 64*, 104.
26. Massey, V., and Williams, C. H., Jr. (1965) *J. Biol. Chem. 240*, 4470−4480.
27. Kanzok, S. F., Schirmer, R. H., Turbachova, I., Iozef, R., and Becker, K. (2000) *J. Biol. Chem. 275*, 40180−40186.

BI0029144